Design and optimization of rheology, strength, and microstructure of quaternary blended self-compacting mortar containing nano silica

Abstract

This paper presents an optimal design range for rheological properties of self-compacting mortar (SCM) through mini slump and v-funnel tests by optimizing the influencing components of the mix design using Taguchi method. Concurrent design of rheology and strength was also considered in the design methodology to reach the highest strength, while maximizing the cement replacement with micro/ nano admixture. For this aim, the influencing factors for rheology and strength were taken into account in two phases of design as binder content (BC), water to binder ratio (w/b), superplasticizer (SP), and limestone powder (LSP) percentage, Slag (S), and nano silica (NS), with each being designed at 4 levels. Two main factors i.e. economical and practical aspects were considered for the levels selection of the variables in Taguchi design. It was found that Taguchi method can be used to come up with a practical and economical design range for rheology of SCM in terms of the mix design components. Yield stress ($\tau 0$) of the SCM mixes was also calculated according to the slump flow diameter obtained form the experiment. Mix design optimization for strength was also implemented and validated for microstructure through SEM images. Laser particle size analyzer (LPSA) along with FE-SEM was also used to investigate the particles' size and, based on which a virtual microstructure was developed to explain the rheological and packing behaviors.

Keywords: self-compacting mortar (SCM), rheology and strength design, micro/ nano admixture; optimization, Taguchi method, virtual microstructure

Research Significance

In this research, design of experiment and Taguchi method was employed to design and optimize a quaternary blended self-compacting mortar incorporating nano silica for rheology and strength. Experimental assessment and parametric study were fully implemented. schematic virtual microstructure was also developed to simulate and demonstrate the shape of the different powdery particles in the mortar mix.

1. Introduction

By definition, self- consolidating concrete (SCC) or self- consolidating mortar (SCM) a composite material that flows due to its own weight, filling the spaces in formwork and passing between congested reinforcing bars under self-weight, and without any means of compaction [1,2]. Hence, what differentiates SCC from other types of concrete is the workability or rheological properties which is its main characteristic to which the mechanical and durability properties are bound. This can be particularly important when it comes to the design of this composite materials with a variety of ingredients which can be different parts of the world. The rheological properties of SCC or SCM highly depends on its constituent materials and mixture composition [3].

There are several studies reporting the influence of ingredients on rheological, mechanical and durability properties of SCC and SCM. However, a more comprehensive formulation approach or design range of rheological properties seems to be missing in materials and design realm of current literature which can be of significant practical value in cement-based materials. Most of the available studies have focused on limited and separate aspects without a more comprehensive design approach. Some studies have assessed the effects of mineral admixtures on SCM and SCC. Santamaria et al. [4] studied the workability properties of SCC containing arc-furnace steelmaking slag as aggregate.

Amini et al. [5] investigated the effect of fly ash (FA) and metakaolin (MK) on time-dependent stability characteristics of SCM under prolonged agitation. Safiuddin et al. studied the effect of rice husk ash (RHA) along with water–binder (w/b) ratio and high-range water reducer (HRWR) on mortars formulated from SCC [6]. Le and Ludwig [7] investigated the effect of rice husk ash and some other mineral admixtures on self-compacting high performance concrete. Jalal et al. [8-11] studied the effect of various nanomaterials and mineral admixtures on rheological, mechanical and durability of SCC .

Khaleel et al. [12] evaluated the influence of various percentages of powders such as FA and MK on SCM workability in 33 mixes. Mahdikhani et al. [13] developed a new method for measuring rheological properties of SCM. A methodology was reported by Nepomuceno et al. [14] for mix design of mortar phase of SCC incorporating binary blends of mineral admixtures. A theoretical model was proposed by Wu et al. [15] for SCC based on rheological properties of the paste. They also developed a new mix design method based on the theoretical model and experimental results. Workability of prestressed SCC in terms of plastic viscosity and yield stress was investigated by Long et al. [16] in order to develop a mix design proportions.

As can be seen from all the studies mentioned herein and others found in the literature, some parameters have separately been studied in specific cases which may not provide an engineer with a clear and insightful idea of what the rheological design range can be based on influencing parameters. This complexity, which is typically found in engineering applications, can be overcome by design of experiment in terms of the influencing parameters and different levels of each that can be done through Taguchi method. This approach

can give an acceptable estimate of design range for the rheological properties based on the main influencing parameters.

Therefore, based on the need for a design range of rheological properties, this study was undertaken. Strength optimization was also carried out using Taguchi method with high cement replacement by micro/ nano admixtures.

Since SCC needs higher amount of paste and as a result powder, the cement content in most of the studies is generally high, thus, as another goal of this study towards CO2 foot print reduction and sustainability in materials and design, it was tried to design the rheological properties while minimizing the cement content and maximizing the cement replacement by waste powders in order to achieve a greener product. Strength optimization was also implemented in terms of various micro/ nano admixture and validated through the experiment. Micro structure of the admixtures was also investigated through particle size analysis and FE_SEM images in terms of size and shape respectively. A virtual microstructure was also developed based on the admixtures' particles size and shape to explain the rheological and packing properties.

2. Materials

2.1. Aggregates

Since this study deals with self-compacting mortar (SCM), the aggregated used was fine aggregates which is sand. The sand was graded according to ASTM C136 and its gradation curve is displayed in Fig. 1.

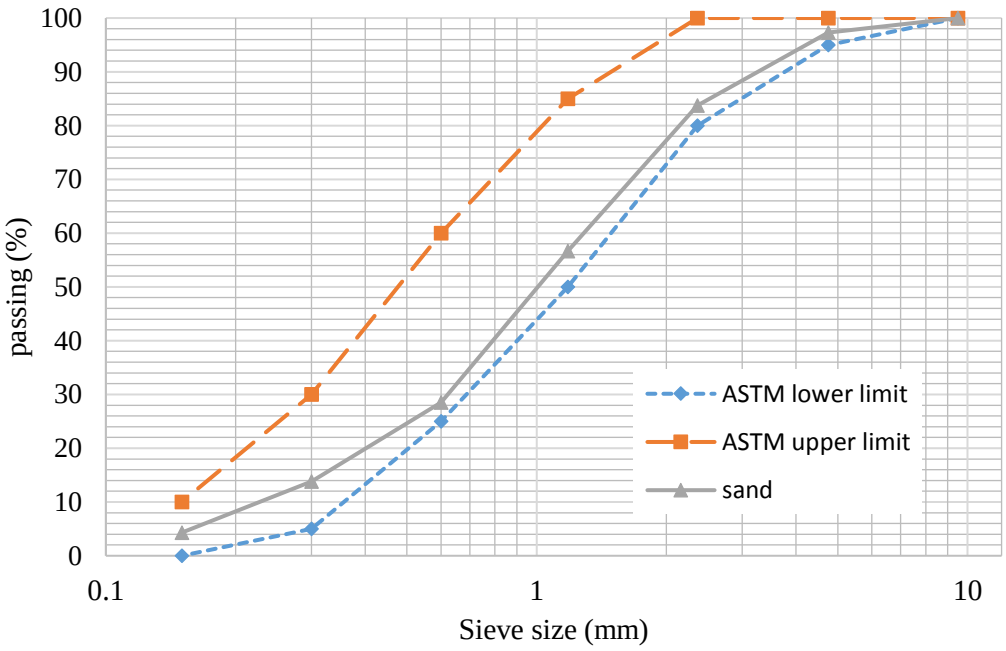

Fig.1. Gradation of the sand used

The specific gravity and water of the sand was determined conforming to ASTM C128 [17] which were measured as 2660 kg/m3 and 2.4% respectively.

Sand fineness modulus

Fineness modulus (FM) is an index indicating the fineness degree of the sand. The larger the FM, the coarser the aggregates particles would be. According to ASTM C125 [18], FM is calculated by using the following equation:

$$F.M. = \frac{\sum(cumulative\ percentage\ retained\ on\ specified\ sieves)}{100} \quad (1)$$

FM is used for fine aggregates and ranges between 1.3 and 3.2. In this study, a sand with FM=3 was used to make the concrete samples.

2.2. Cementitious materials

Cement

Cement type II was used in this study. The properties of the cement used along with the recommended values by ASTM C150 are presented in table 1.

Table 1. Physical and chemical properties of the cement

Chemical composition (%)			Physical characteristics				
Component	%	ASTM C150 limit (max)	Characteristics		Unit	Result	ASTM C150 limit
MgO	1.946	6	Specific surface area		cm2/g	3050	_
Na2O	0.075	_	Time of setting (Vicat test)	Minute	140	45	_
SiO2	17.04	_		Minute	210	375	_
Al2O3	3.697	6	Specific gravity		g/cm3	3.14	_
P2O5	0.124	_	Autoclave expansion (max)		%	0.1	0.8
SO3	4.125	3	Compressive strength (min)	1 day	kg/cm2	95	_
K2O	0.791	_		2 day	kg/cm2	170	_
CaO	64.896	_		3 day	kg/cm2	210	100

TiO2	0.267	_	7 day	kg/cm2	310	170
MnO	0.12	_	28 day	kg/cm2	440	280
Fe2O3	3.443	_	60 day	kg/cm2	500	_
LOI	2.62	3				
SrO	850 ppm	_				

Fly Ash (FA)

Class F fly ash was used as one of the cementing materials for partial replacement of the cement in this study. The color of the FA powder is light gray and its specific gravity is 3200 kg/m3. Particles are spherical and 90% of the particles are 45 μm in size. The chemical properties of the FA used are summarized in table 2.

Table 2. Properties of class F fly ash

MgO	Al2O3	SiO2	P2O5	K2O	CaO	TiO2	Fe2O3	Cr2O3	Specific gravity (g/cm3)
0.96	23.54	65.08	0.51	1.04	1.54	1.94	4.27	0.12	2.3

Slag (S)

The slag used in this study was of 2790 kg/m^3 specific gravity and 83% passing the sieve #200. Its specific surface area was measured as 4200 cm2/g. Presented in table 3 are the chemical properties of the slag obtained by XRF.

Table 3. Chemical analysis of slag obtained from XRF test

Oxides	%
MgO	2.32
Al2O3	7.31
SiO2	38.22
P2O5	0.51

SO3	6.36
K2O	0.97
CaO	39.11
TiO2	1.17
MnO	1.73
Fe2O3	0.93
Cr2O3	0.12
BaO	0.15

Nano silica

Colloidal nano silica was used in this study, the properties of which are presented in Table 4. The main advantage of colloidal nano silica over the powder one is that its dispersion would be less of an issues, which makes the results more reliable.

Table 4. Properties of colloidal nano silica

Specific gravity (g/cm^3)	Particle size (nm)	Viscosity (pa s)	Solid content (Wt. %)	PH	Specific surface area (m^2/g)
1.386 _1.403	40_60	Max 15	49_50.5	9.5	70 _ 100

Superplasticizer (SP)

Superplasticizer of a specific type is an inseparable part of SCC and SCM mix design. To make the self-compacting mortar mixtures, Polycarboxylate based super plasticizer was used. It was a liquid with light brown color and specific gravity of 1.1 kg/m3

3. Methodology

The purpose of this study is to formulate and optimize the design range of rheological properties of SCM in order to develop a more global and comprehensive approach for the rheology design. With this respect, several aspects were taken into account. It was tried to maintain a trade-off among all the aspects through the optimization by Taguchi method. Considering the CO2 foot print and sustainability in materials and design, it was also aimed to maintain the cement content as practically low as possible in the first phase, and cement replacement with various admixtures in the second phase. Thus, the goals of the design can be summarized as the following:

- Determination of practical ranges of the influencing parameters.
- To keep the main two rheology measures i.e. mini slump diameter and v-funnel time in the range of 20- 30 cm and 5- 10 s respectively.
- Minimization of cement content and w/b ratio for reducing the environmental impact, and enhancing the mechanical and durability properties of SCM, respectively.

Two main phases including three steps were undertaken to achieve the goals:

Phase A: designing the basic mix of SCM for rheological properties.

Step 1. Preliminary (rough) design of the basic mix for influencing factors and levels.
Step 2. Final design of the basic mix for the factors' level, and selection of the best option based the goals (criteria)

Phase B: designing the final mix of SCM with admixtures.

Step 3. Designing the final mix based on the admixture factors and their levels.

The influencing factors for rheological properties of SCM were selected as water/ binder (w/b) ratio, super plasticize (SP), limestone powder (LP), binder content (BC). Rheological properties were measured through slump flow diameter and v-funnel time, with the former being considered primarily in Taguchi method for the design range. In order to investigate the synergic effect of various admixtures on rheology, two mineral admixtures i.e. fly ash (FA) and Slag (S), and one nanoparticle i.e. Nano silica (NS) were selected for phase B of the design. In the phase B, concurrent design of strength and rheological properties was considered in order to investigate the effect of admixtures on rheology and strength. In this approach, the rheology is intended to be designed for slump flow diameter and controlled by v-funnel time, as well as stability control through the visual inspection.

4. Taguchi method for design

Taguchi methodology for optimization can be divided into four phases: planning, conducting, analysis and validation. Each phase has a separate objective and contributes towards the overall optimization process. Taguchi's methods focus on the effective application of engineering strategies rather than advanced statistical techniques [19].

In order to predict the results of the experiment designed by Taguchi method, Eq. 2 is used:

$$\eta = \eta_m + \sum_{i=1}^{f}(\eta_i - \eta_m) \quad (2)$$

Where, η_m is the overall mean value of all Signal/Noise (S/N) ratios in all experimental runs, f is the number of factors, and η_i is the mean of S/N ratios corresponding a factor levels [20, 21]. In order to calculated the optimum results, the equation can be written as:

$$\eta_{opt} = \eta_m + \sum_{i=1}^{f}(\eta_{i-opt} - \eta_m) \quad (3)$$

Where, η_{opt} is the mean of S/N ratios corresponding to the factors' optimum levels.

Taguchi method was applied to design the experiment for rheological properties at three steps: steps 1 and 2 of the phase A, and step 3 of phase B. tables 5a and b shows the factors and the levels for the steps 1 and 2, respectively.

Table 5. Factors and levels of phase A of rheology design

(a)

factors (step 1)	level 1	level 2	level 3	level 4
w/b ratio	0.37	0.4	0.45	0.5
SP%	0.9	1.2	0.6	0.3
LSP%	10	20	0	15
Binder content	650	600	700	550

(b)

factors (step 2)	level 1	level 2	level 3	level 4
w/b ratio	0.3	0.35	0.4	0.45
SP%	0.9	1.2	0.6	0.3

LSP%	10	20	0	15
Binder content	650	600	550	700

The range of the factors in the preliminary design was selected in such a way to cover the typical minimum and maximum values reported in the literature, considering also the practical aspects of the workability. For example, the w/b ratio was not selected too low, as it may not be suitable for practical applications. Therefore, the levels of the factors w/b, SP, LP, and BC were selected as presented in table 5a. It is worth emphasizing that determination of the maximum and minimum of the factors is momentous in order to achieve the goals of the study.

Based on the results obtained from preliminary design in step 1 which are presented in "results and discussion" section, adjustments of the levels were made which are reflected in table 5b. Several aspects were considered for levels' adjustment including practical workability, cement content minimization, and cement replacement.

Once the phase A of design is implemented and the optimum levels of the basic factors are determined, the basic mix design is complete, based upon which the final mix with admixtures can be designed. Table 6 presents the factors and levels used in phase B for the final mix design of the SCM mix for the rheological and strength properties.

Table 6. Factors and levels of phase B of the design

SCM	Level 1 (%)	Level 2 (%)	Level 3 (%)	Level 4 (%)
flay ash	0	10	20	30
slag	0	10	20	30
Nano Sio2	0	2	4	6

In order to investigate the mechanical properties of the mixes design with Taguchi method, the last design was also considered for mechanical properties to optimize the strength of the SCM samples. With a concurrent deign of mechanical and rheological properties, it can be observed that what rheological properties the optimized mixes would result in. in fact with the concurrent design, a cross validation can be made to make sure the mechanically optimized samples have also a desirable range of rheological properties.

5. Rheology and yield stress

Mortar and paste play a major role in the rheological properties of self-compacting concrete. For a given cementitious material in the fresh state, the yield stress and the plastic viscosity are generally considered the two most important rheological properties in terms of workability. [22]. The rheological parameters characterizing the workability of the cement paste are the yield stress "τ0"which corresponds to the stress required to initiate flow and the plastic viscosity "μ" which describes the paste resistance to flow under external stress. [23]. Yield stress is the minimum stress for irreversible deformation and flow of any material which behaves like a fluid, such as concrete or mortar. It is a very important factor for Self-consolidating concrete and mortar, which have high fluidity [24]. The yield stress of concrete or mortar can be measured by rheometry, but it is very expensive and complex for construction site [25]. Thus, many researchers have investigated the yield stress and plastic viscosity by linking the slump-cone and v-funnel test, which is simpler and cheaper for practical purposes. Some studies have investigated the correlation between plastic viscosity to mini-slump and v-funnel time under boundary condition such as time of spread and the characteristics of the flow final profile [26-28].

The following equation [25] was used to calculate the yield stress from the slump flow diameter which was used in this study.

$$\tau_0 = \frac{225\rho g V^2}{128\pi^2 R^5} \qquad (4)$$

6. Experimental procedure

The experimental procedure included mixing, measuring the rheological properties, and also strength tests of the mortar samples. For mixing purpose, first all of aggregates and powder materials were mixed in a mixer for another one minute. After that, 80% of the needed water was added and mixing was performed for one minute. The remaining water, superplasticizer, and colloidal Nano silica were mixed together and added to the mixture and mixed for another one minute. Then having given the mixture a rest for 100 s, it was mixed for another 30 s at higher speed. A view of the mortar mixing device is displayed in Fig. 2.

Fig. 2. A view of mortar mixer machine

Rheological tests for self-compacting concrete and mortar are outlined in ASTM C1611 and EFNARC [1, 29]. Two tests were carried out to measure the rheological properties of the mortar, namely mini slump and V-funnel, as illustrated in Fig. 3.

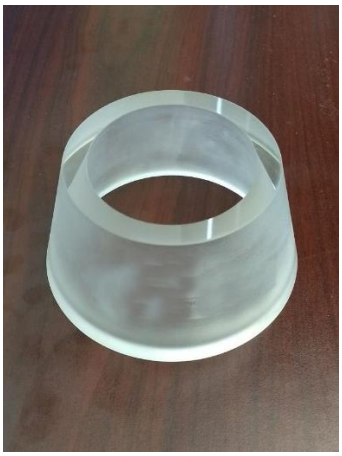

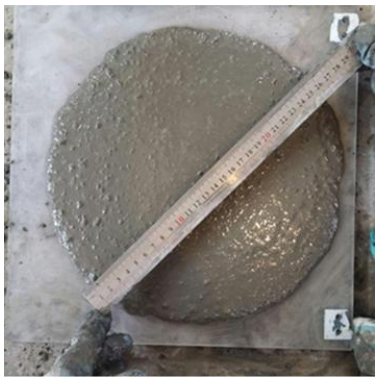

(a) (b)

Fig. 3. Tests for fresh properties of mortar: (a) mini slump, (b) v-funnel

Visual inspection of rheological properties was also exercised conforming ASTM C1611, as described in table 7.

Table 7. Visual stability inspection (VSI) values as outlined in ASTM 1611 [29]

VSI value	Criteria
0 = Highly Stable	No evidence of segregation or bleeding.
1 = Stable	No evidence of segregation and slight bleeding observed as sheen on the concrete mass.
2 = Unstable	A slight mortar halo ≤ 10 mm [≤ 0.5 in.] and/or aggregate pile in the center of the concrete mass
3 = Highly Unstable	Clearly segregating by evidence of a large mortar halo > 10 mm [> 0.5 in.] and/or a large aggregate pile in the center of the concrete mass

The mortar samples for strength tests were prepared according to ASTM C109 as 5*5*5 cubes which were cast without vibration or tamping. Then the samples were covered with a wet sheet. The samples were demolded after 24 hours and stored in saturated lime water at 21◦C until the test day.

7. Results and Discussion

7.1. Rheological properties

Test results of the preliminary design of phase A for mini slump diameter, along with the v-funnel time and visual inspection results are presented in table 8. It can be seen that the diameter results range between 10 cm and 38.5 cm. As is noted from the results, 80% of the preliminary mixes show acceptable results without instability including segregation and bleeding.

Table 8. Results of rheological properties of step 1 of phase A of design

Mix No. (step 1)	**W/B**	**SP %**	**LSP%**	**Binder content**	**Slump (cm)**	**V-funnel (s)**	**VSI**

A-1-1	0.37	0.9	10	650	27.5	4.5	0
A-1-2	0.37	1.2	20	600	25.5	5	0
A-1-3	0.37	0.6	0	700	22.5	4.81	1
A-1-4	0.37	0.3	15	550	10	B*	B
A-1-5	0.4	0.9	20	700	33	1.78	3
A-1-6	0.4	1.2	10	550	23.5	5.2	0
A-1-7	0.4	0.6	15	650	24.5	4.1	0
A-1-8	0.4	0.3	0	600	12.5	32	B
A-1-9	0.45	0.9	0	550	26	4.53	1
A-1-10	0.45	1.2	15	700	38.5	1.5	3
A-1-11	0.45	0.6	10	600	25	3.03	1
A-1-12	0.45	0.3	20	650	15	3	NF**
A-1-13	0.5	0.9	15	600	37.5	1.84	3
A-1-14	0.5	1.2	0	650	38.5	12.8	3
A-1-15	0.5	0.6	20	550	26	2.47	1
A-1-16	0.5	0.3	10	700	27	1.3	2

*B: Blocking

**NF: Not flowing

The results obtained also indicate that the lower limit for cement with respect to cement minimization goal, can be taken as 600 kg/m3. It is also noticed that some of the mixes with acceptable slump flow do not meet the v-funnel requirements. The effect of LP on consistency enhancement of the SCM mixes was also observed in the tests. The results also indicate that the levels of SP have not pushed the rheological measures outside the desirable range which proves the appropriateness of the levels selected. It was observed that 80% of the mixes were in an acceptable range and did not show any bleeding or segregation.

Due to significance of w/b ratio on rheological behavior of the SCM, the range of this parameter was changed to a lower range as 0.30- 0.45 in the second step of the design. Reported in table 9 are the results of the step 2 of the design.

Table 9. Results of rheological properties of step 2 of phase A of design

Mix No. (step 2)	**W/B**	**SP %**	**LSP %**	**Binder content**	**Slump (cm)**	**v-funnel (s)**	**VSI**

A-2-1	0.3	0.9	10	650	10.5	B	B
A-2-2	0.3	1.2	20	600	16	140	B
A-2-3	0.3	0.6	0	550	10	B	B
A-2-4	0.3	0.3	15	700	10	B	B
A-2-5	0.35	0.9	20	550	11.5	B	B
A-2-6	0.35	1.2	10	700	29	4.35	1
A-2-7	0.35	0.6	15	650	10	B	B
A-2-8	0.35	0.3	0	600	10	B	B
A-2-9	0.4	0.9	0	700	31.5	3	3
A-2-10	0.4	1.2	15	550	24	5.4	B
A-2-11	0.4	0.6	10	600	14.5	B	B
A-2-12	0.4	0.3	20	650	10	B	B
A-2-13	0.45	0.9	15	600	29	2.4	3
A-2-14	0.45	1.2	0	650	32.5	1.8	3
A-2-15	0.45	0.6	20	700	38	1.3	3
A-2-16	0.45	0.3	10	550	10	B	B

As is vividly understood from the table, 11 out of 16 mixes, i.e. about 70%, either did not flow in slump test or faced blocking the v-funnel test. As a results, it was concluded that the first step of the design was good enough to proceed with, and the second step can be stopped. The only parameter changed in this step that can significantly affect the performance of the mortar I terms of strength and durability, and is intended to be minimized is w/c ratio. It can be concluded from the table that w/b=0.3 is basically not a practical choice, however, the next lowest level i.e. w/b=0.35 can be a feasible option, depending on the combination of other factor which can be deduced from the parametric study analysis. Bae on the obtained results, it was found that the slump flow diameter for the basic mix without can be optimally in the range of 23-28 cm with an average around 26 cm. the purpose of finding this range or average for the basic mix is to make sure that if the plain concrete without mineral admixture is used, the rheology is good enough, and in the case of incorporation of various admixtures, the range allows an acceptable tolerance of the rheology variation so that a desirable workability can be reached, while maintaining an enhanced mechanical and durability properties.

7.1.1. Parametric study of phase A of design

In order to analyze the results of the rheological properties obtained for the basic mix design, a parametric study is necessary to determine the practical ranges of the slump according to different levels of the factors. As mentioned earlier. W/b=0.3 was not feasible and hence, the focus would be placed on next lowest level which is 0.35. Fig. 4 displays the results of the step 2 of the design for different levels of the variables for constant w/b=0.35. It can be clearly seen from the pictures that by increasing the SP amount, the rheology curves shift upward until they reach the desirable design range.

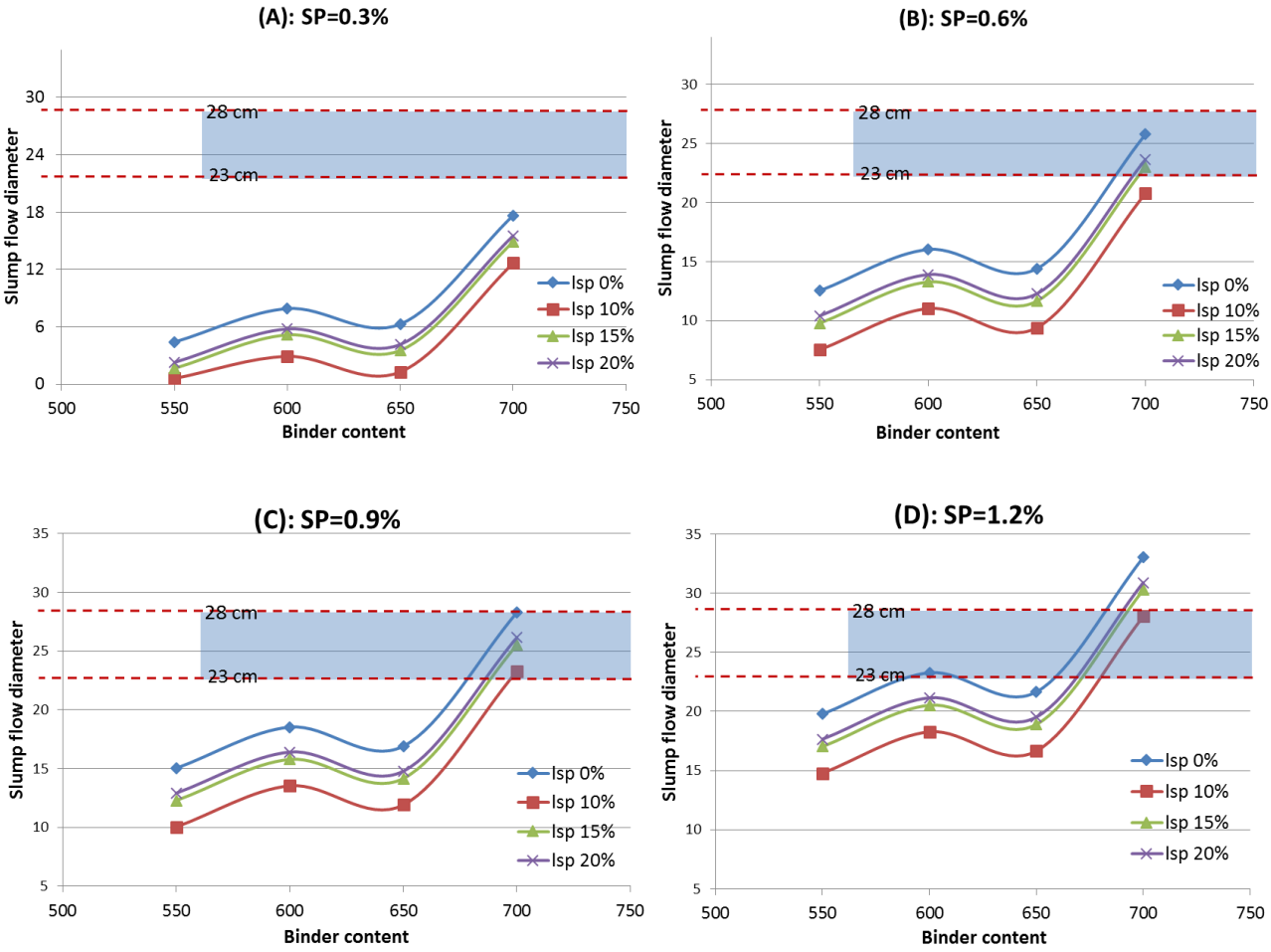

Fig. 4. Results of the step 2 of the design for different levels of the variables for constant w/b=0.35

As is noted, broader areas of the curves are covered by design range at SP=1.2% and hence, the combination of w/b=0.35 and SP=1.2% can be taken as the optimal values for the two parameters so far. Especially, binder content 600 kg/m3 reaches the design range at SP=1.2% which allows the selection of possible lower binder content.

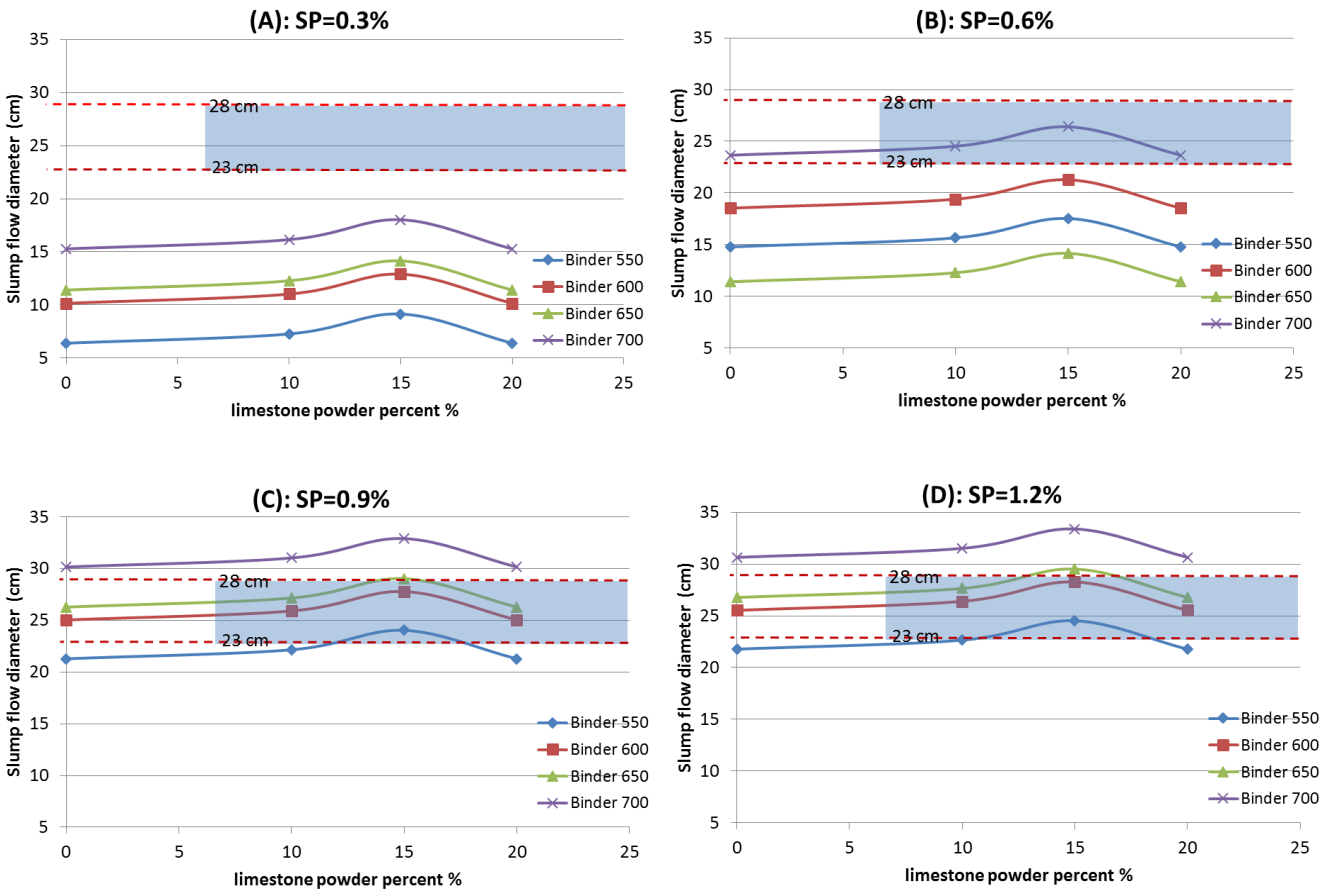

Fig. 5. Variation of the slump flow versus LSP% for different binder contents at different levels of SP%

While w/b and SP% meet our design goals and can be selected at this step, nonetheless, they can still be investigated more through the parametric study of the first step, along with the other two parameters, i.e. binder content (BC) and LSP%. In this respect, parametric study of rheology design using Taguchi method is presented in the following figures. Fig. 5 shows the variation of the slump flow versus LSP% for different binder contents at different levels of SP%, by taking constant w/b= 0.37. As is seen clearly form the plots, SP=0.9% and 1.2% both can reach the design range. Nevertheless, since the plot presented earlier show that 1.2% is a more optimal option, SP=1.2% can be taken as the best choice. It is also noted from this figure that at the binder content of 600 kg/m3 with SP=1.2%, the rheology can reach to the design range which satisfies the goal of practical minimization of binder content, and as a result cement content reduction.

It can be deduced form Fig. 5 (C) and (D) that even though there is an obvious optimum value for LSP% at 15%, nevertheless both LSP=15% and 20% fall in the design range, with LSP=20% being closer to the average value of the slump range (26cm), and higher replacement level. Consequently, LSP=20% can be chosen as the best design option according to the design goals.

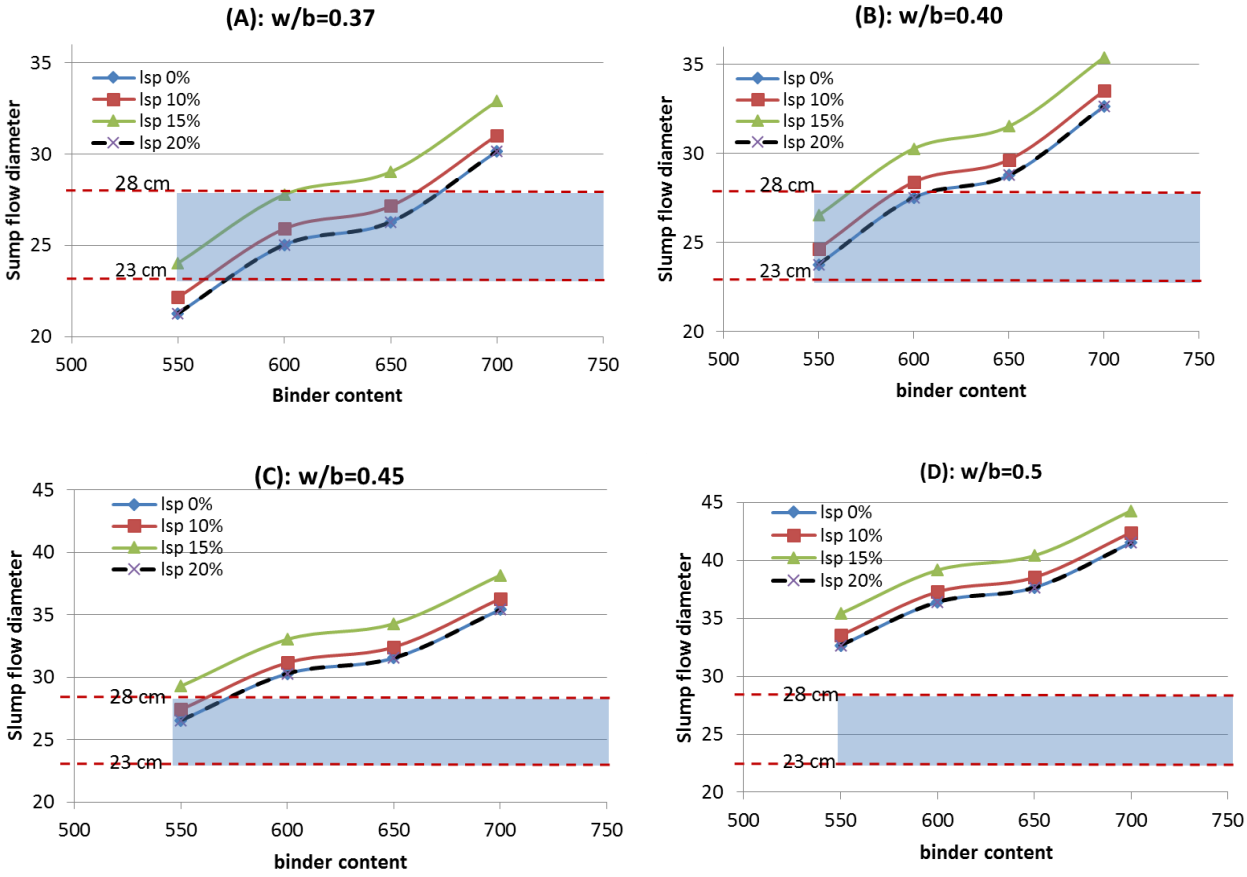

Fig. 6. influence of w/b ratio and binder content at a constant SP=1.2%

The influence of w/b ratio at a constant SP=1.2% is demonstrated in Fig. 6. As can be seen, increasing the w/b ratio dramatically increases the slump flow which can lead to severe bleeding and segregation. It is noted from Fig. 6 (C) and (D) that by increasing the w/b ratio, rheology curves can mostly move out of the design range. However, the best situation is observed for the lowest w/b in plot (A), where the rheology curves fall in the design range.

7.1.2. Results and parametric study of phase B of design

Once the basic mix was designed in phase A, the final design was implemented by incorporating micro and nano admixtures in phase B. it is worth mentioning that in fact, a concurrent design of rheological and mechanical properties was implemented in phase B using Taguchi method. Even though the focus of this study was on rheological properties, nonetheless the strength deign was also taken into account to see what mechanical properties the optimal design range of rheology would result in. table 10 reports the rheology results of the phase B of design. As mentioned earlier, four levels of micro and Nano admixtures

were considered; FA and slag as the former and NS as the latter. It is noted from the table that by adding micro admixtures up to 30% and Nano admixtures up to 6%, the slump flow varies between 23.6 cm and 25.9 which is pretty close to the average of design range determined in the prior phase. V-funnel time also varies in the range of 6.4- 8.9 s with average of 7.4 s which coincides well with the average of the design range, i.e. 5-10 s. According to the results, visual inspection of the mixtures also proved a perfect stability of the mixes of phase B, which demonstrates the robustness and validity of the prior phase of the design for the basic mix.

Table 10. Rheology results of the phase B of design

Mix No.	Mix ID (phase B)	FA (%)	Slag (%)	NS(%)	slump diameter (cm)	V-funnel time (s)
B-1	MF0S0NS0	0	0	0	25.7	8.9
B-2	MF0S10NS2	0	10	2	25.5	6.5
B-3	MF0S20NS4	0	20	4	24.5	7.8
B-4	MF0S30NS6	0	30	6	25.9	6.5
B-5	MF10S0NS2	10	0	2	25.5	6.98
B-6	MF10S10NS0	10	10	0	25.7	8.5
B-7	MF10S20NS6	10	20	6	24	8
B-8	MF10S30NS4	10	30	4	25.5	7
B-9	MF20S0NS4	20	0	4	24.5	6.4
B-10	MF20S10NS6	20	10	6	24	7.03
B-11	MF20S20NS0	20	20	0	24.5	7.9
B-12	MF20S30NS2	20	30	2	24	7.7
B-13	MF30S0NS6	30	0	6	23.6	8.5
B-14	MF30S10NS4	30	10	4	25.5	6.9
B-15	MF30S20NS2	30	20	2	24.5	6.6
B-16	MF30S30NS0	30	30	0	23.7	7.7

Parametric study of the rheological properties of the final mix containing admixtures is presented in the following figures. As mentioned earlier, the influence of two micro and one nano admixtures was investigated in this phase. Fig. 7 shows effect of NS and Slag variations on slump flow, at constant levels of FA replacement. It can be seen that from the 3D plots that higher slump flow is predicted at 4% and 10% of NS and Slag respectively, at different levels of FA replacement. However, the effect of 0% and

30% of slag on the rheology seems to somewhat close, less than the corresponding value of slump flow for 10%.

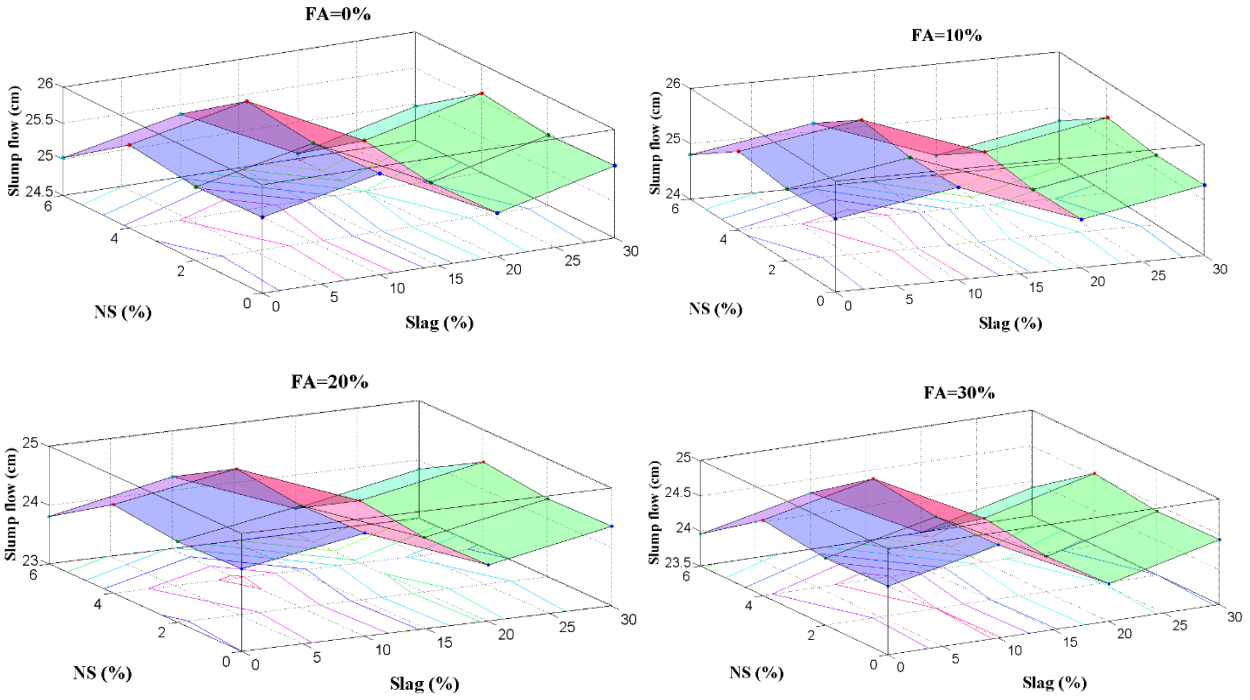

Fig. 7. Variation of slump flow vs. NS (%) and slag (%) at constant FA% for different replacement levels

Plots presented in Fig. 8. Show the synergic effect of NS and FA on the slump flow, at various level of Slag. What is noted from the prediction plots is the fact that FA increase, has reduced the rheology a little, with an optimum amount of 10%. Nevertheless, the change of rheology at different replacement level is not significant. This prediction result for FA is rather contradictory to the earlier findings regarding its single effect on the rheology as an increasing factor [2]. It can be attributed to the synergic effect of different powders, as 20% of LSP is already incorporated in the basic mix design, when FA is added to the final mix in phase B. nevertheless, it should be noted that due to the appropriate design of phase A, the rheology change due to FA in this phase is not considerable.

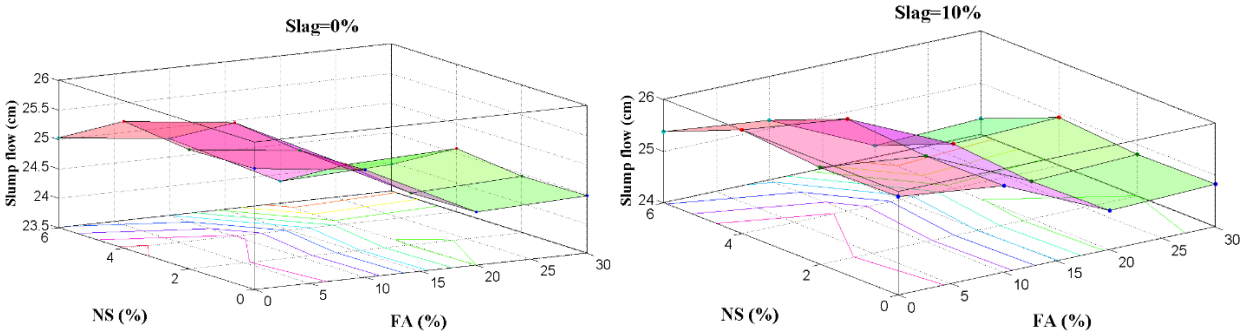

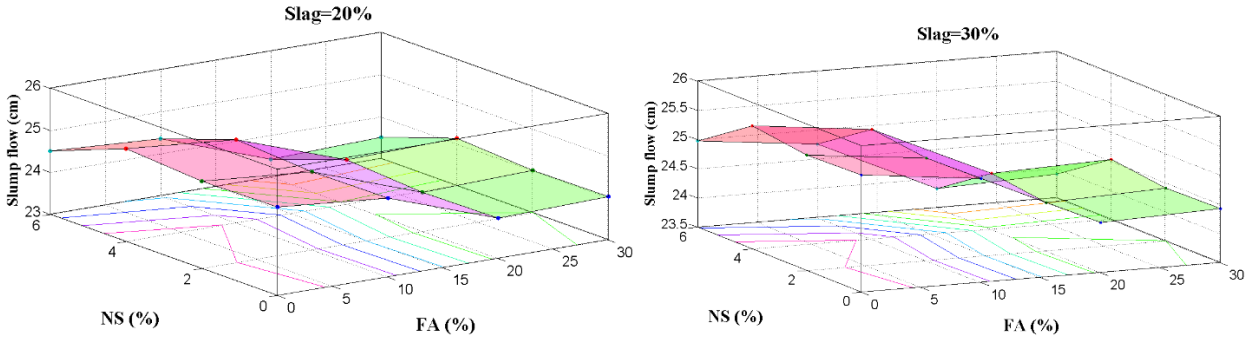

Fig. 8. Varication of slump flow vs. NS (%) and FA (%) at constant Slag% for different replacement levels

The influence of Slag and FA percentage on rheological properties at various levels of NS is depicted in Fig. 9. According to the plots, the minimum rheology of design phase B turned out to be at 20%, 20% and 6% of Slag, FA, and NS respectively, with slump flow of about 23.5 cm.

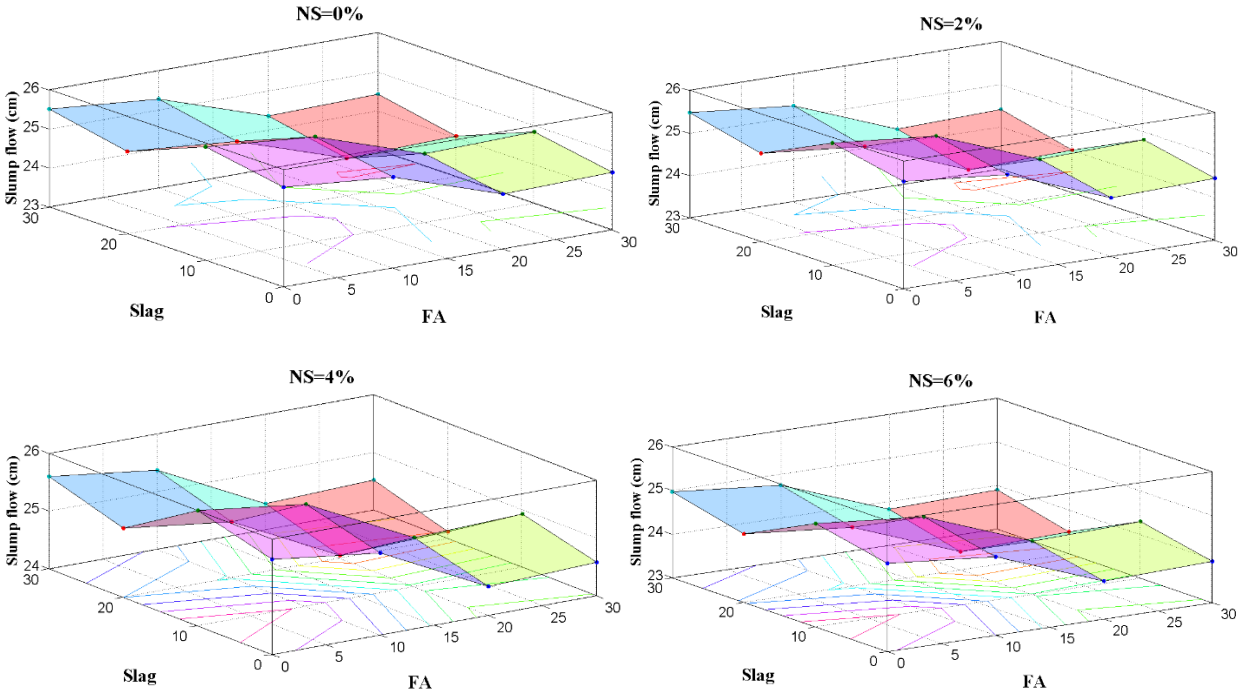

Fig. 9. Varication of slump flow vs. FA (%) and slag (%) at constant NS% for different replacement levels

7.2. Strength results of Taguchi design

The strength results of Taguchi design for strength are plotted in Fig. 10 for two ages of 14 and 28 days. Once the results were obtained, the analysis and optimization were carried out to maximize the compressive strength. The output of Taguchi optimization for micro and nano admixtures are displayed in Fig. 11. As can be seen from the figure, the optimum percentages occur at 20%, 20%, and 4% of slag, FA, and NS respectively. In order to validate the strength results obtained from Taguchi design, three samples were made according to the optimum mix design. Table 11 comparatively summarizes the strength results of the optimum mix, the best mix according to Fig. 9, and the basic mix. It is noted that the optimum mix shows the highest strength, well proving the robustness of the design and optimization.

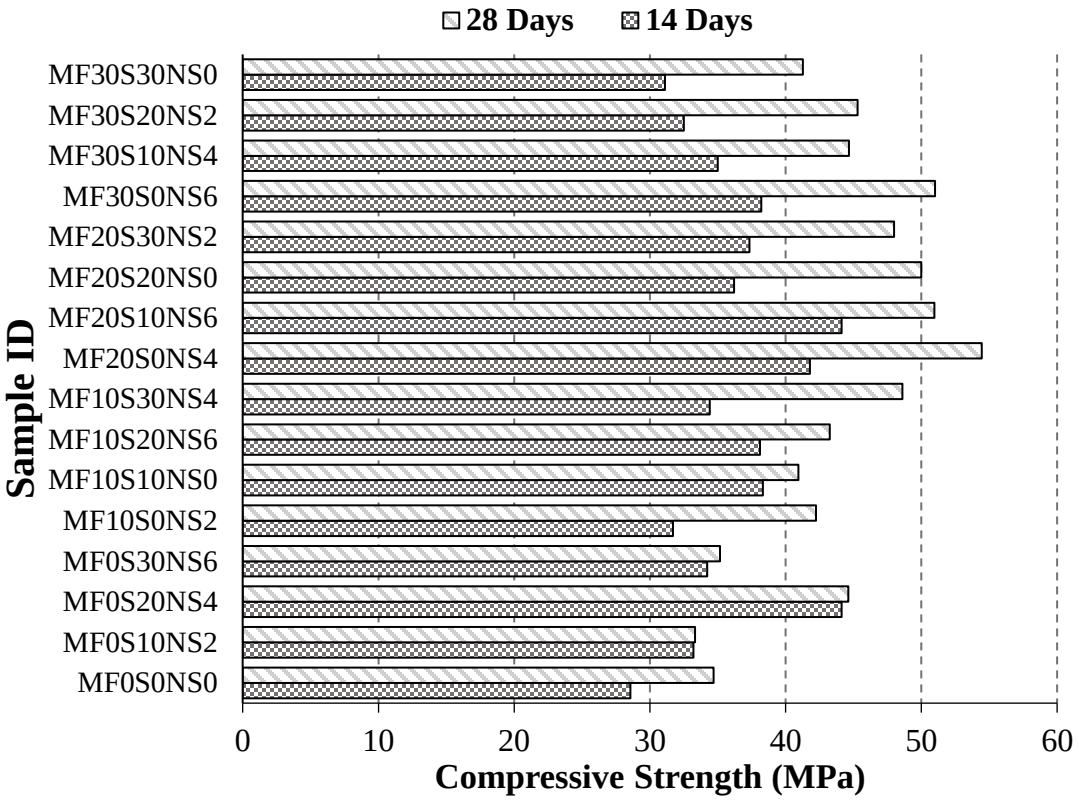

Fig. 10. Strength results of mixes designed by Taguchi method

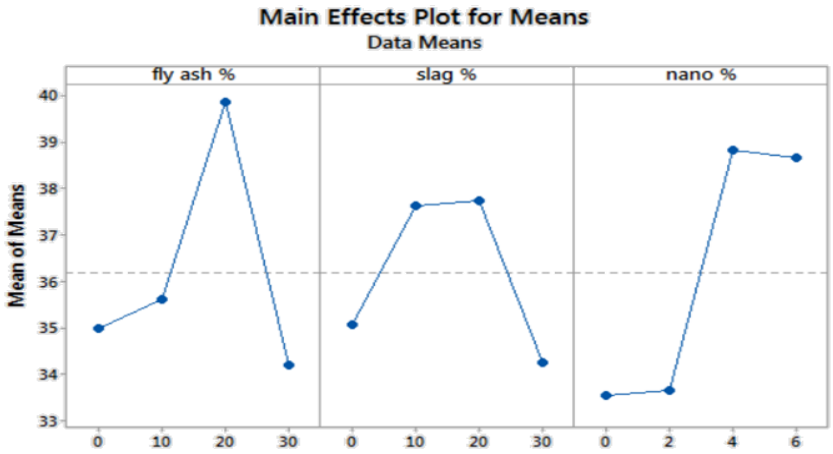

Fig. 11. Optimum results of Taguchi design

Fig. 11. Comparison of the basic mix, the best mix in the design, and the optimum mix

Sample Name	w/b	Binder content	LSP (%)	FA (%)	Slag (%)	Nano Sio2 (%)	slump diameter	V-funnel time (s)	Strength (MPa)
Basic mix	0.35	600	20	0	0	0	25.7	8.9	34.69
MF20S0NS4	0.35	600	20	20	0	4	24.5	6.4	54.44
Opt mix	0.35	600	20	20	20	4	24	7.5	54.60

In order to compare and identify the difference between the basic mix and the optimum one designed by Taguchi method in this study, the SEM micrograph of both mixes at 28 days of age are illustrated in Fig. 12. A more refined microstructure with less porosity can be vividly seen I the image. It can be attributed to the simultaneous effect of micro and nano admixtures, especially at optimum levels of replacement which can from one hand physically enhance the microstructure through particle packing [30], and on the other hand, chemically affect the formation of reaction products due to synergic effects of pozzolanic and nano admixtures.

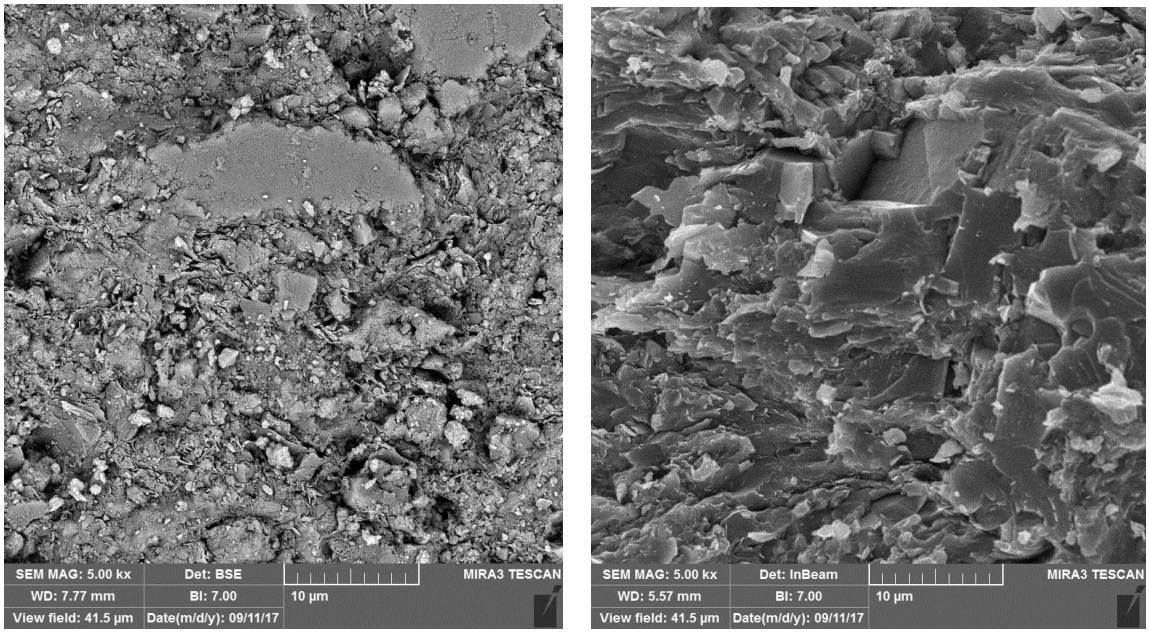

(a) (b)

Fig. 12. SEM images of basic mix and optimum mix

7.3. Yield stress results

Listed in table 12 are the yield stress results obtained from the mini slump test for Phase A and B of the design based on Eq. (4). As is seen from the table, the yield stress values of all mixes range from 1 to 25 Pa except for the mixes with Blocking or Not flowing labels. In fact, the yield stress values out of the mentioned range represent mixes that are inhomogeneous or of very high viscosity.

Table 12. Yield stress results calculated from the slump flow diameter

Phase A of Design																
Mix No.	1-1	1-2	1-3	1-4	1-5	1-6	1-7	1-8	1-9	1-10	1-11	1-12	1-13	1-14	1-15	1-16
Slump D (cm)	27.5	25.5	22.5	10	33	23.5	24.5	12.5	26	38.5	25	15	37.5	38.5	26	27
τ0 (Pa)	8.45	12.64	25.9	1472.6*	3.82	19.03	17.02	490.34*	12.13	1.77	15.76	201.58*	2.01	1.72	12.47	10.21
Phase B of Design																
Mix No.	B-1	B-2	B-3	B-4	B-5	B-6	B-7	B-8	B-9	B-10	B-11	B-12	B-13	B-14	B-15	B-16
Slump D (cm)	25.7	25.5	24.5	25.9	25.5	25.7	24	25.5	24.5	24	24.5	24	23.6	25.5	24.5	23.7
τ0 (Pa)	13	12.97	16.7	12.27	13.57	13.56	18.57	13.82	17.07	18.94	17.36	19.57	21.04	13.72	17.61	21.48

* Large yield stress values are due to Blocking or Not flowing mixes

7.4. Microstructural assessment of rheology and strength

Most of the macro structural observations are resulted from microstructure of the materials which needs to be taken into account in design process. Rheological properties of the SCC and SCM are mainly affected by three factors: liquid materials such as water and SP, aggregate gradation, and powdery materials. Amongst all, the role of paste and powder on rheological properties is more. From microstructure perspective, while liquid ingredients and aggregates may not have much to do with microstructural observations, however, the powdery materials can be very interesting which is worth being investigated in more details. Aside from other possible parameters, two characteristics of the powder particles that can affect the rheology consist of particle size and particle geometry.

Finer particles can improve the consistency of the paste and thereby leading to more homogeneity of the SCM mixture and less bleeding and segregation. They can also better distribute in the liquid phase of the mixture in the spaces among the aggregate particles.

With regard to geometry, the less the angularity of the particles, the better the movement and skidding of the particles on top of each other could be, and hence resulting in less shear stress and more flowability of the mixture. In this respect, two factors can be roughly mentioned as "sphericity" and "angularity". The former can describes how close the particle shape is to a sphere, or the number of faces that a particle has, and the latter pertains to how sharp or smooth the corners and boundaries of the sides are. Schematic representation of the geometry factors are presented in Fig. 13.

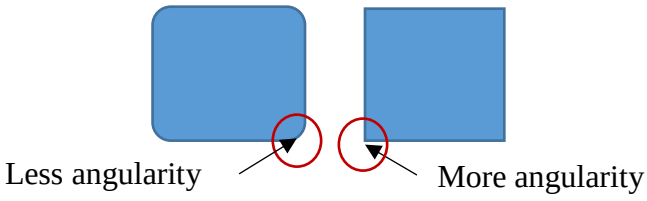

(a)

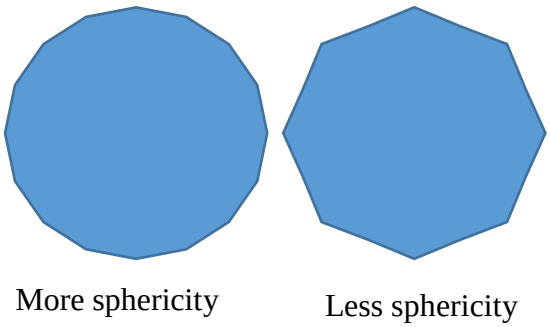

(b)

Fig.13. Schematic representation of particles (a) angularity and (b) sphericity

7.4.1. Size assessment through Particles Size Analyzer (PSA)

Five different types of powders were used in this study namely C, FA, S, LP, and NS, each of which can partially affect the rheology of the mixture. Based on the aforementioned discussion, microstructural assessment of the two influencing factors i.e. particles' size and shape were investigated in this study. Laser particle size analyzer (LPSA) was used to characterize the particle size distribution (PSD) of the micro powders, the results of which are presented in Fig 14. For NS, the upper size range i.e. 60nm was considered for average particle size comparison herein.

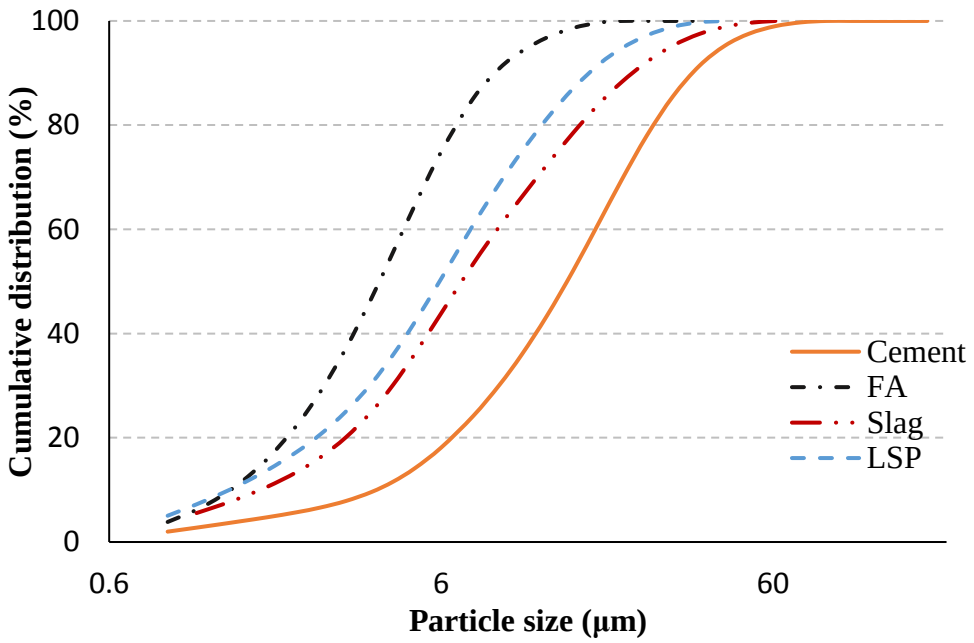

Fig. 14. Particle size distribution (PSD) of the micro admixtures

The mean (μ) and standard deviation (σ) of the particles' size were calculated by the following equations:

$$\mu = \frac{\sum_{i=1}^{k} f_i x_i}{n} \quad (5)$$

$$\sigma = \sqrt{\frac{\sum_{i=1}^{k} f_i (x_i - \mu)^2}{n}} \quad (6)$$

Where, μ is mean, σ is standard deviation, f is frequency, n is sum of frequencies, and k is number of datasets.

For the sake of more clarity and better comparison, mean particle size of all the micro and nano admixtures used are plotted in Fig. 15.

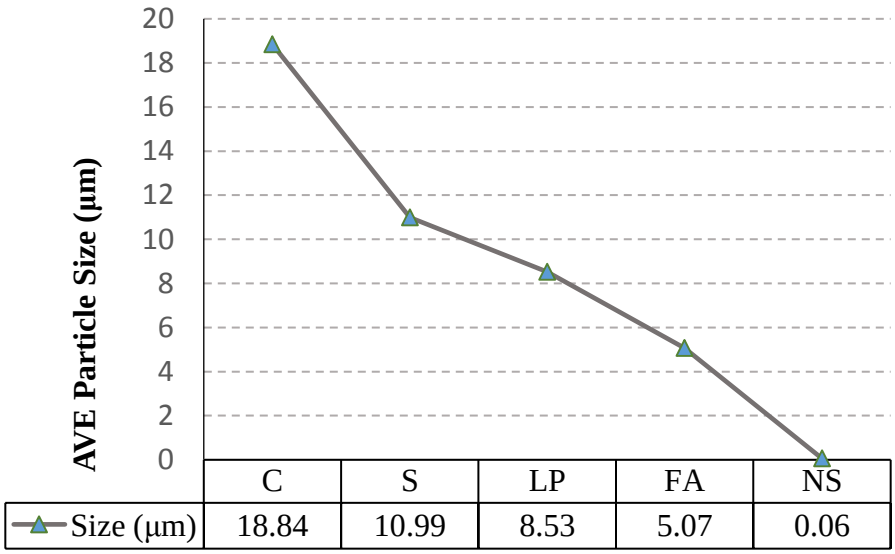

Fig. 15. Mean particle size of all the micro and nano admixtures

As is noted from the figure, the particle size decreases in order from cement to NS. It can be said that particle size role is not as significant as the geometry in rheology. However, combination of different particles sizes can affect the packing, and thereby influencing the workability and consistency of the mix. In strength perspective, though, the particle size effect is definitely significant that in a combinatory state, can lead to improved particle packing [30] and thereby resulting in less porosity and enhanced strength. In this case, a better packing density can lead to a denser microstructure and subsequent higher strength.

7.4.2. Particles geometry assessment

For geometry assessment of the powder particles, FE-SEM micrographs of the powder particles were prepared which are illustrated in Fig. 16. The particles shape and geometry can be roughly identified through the micrographs. For better presentation, the boundary of a sample particle has been marked by a solid line. By visual observations from the micrographs, it can be said that the cement particles have more angularity and their sphericity is comparatively almost the lowest among the powders. After the cement,

the slag comes with lowest sphericity and kind of similar sharpness of the corners and edges of the particles. In the next level, LSP particle as indicated by the solid line, shows more sphericity with smoother edges and less roughness. The best and ideal situation can be observed for FA particles which are perfectly spherical with very smooth surfaces. NS particles are very tiny with spherical geometry, however, due to diminutiveness, the surfaces of the particles are not clear in the image. Besides, some extent of agglomeration can be expected even if they are dispersed well in the mix, which can affect the rheology, in terms of both sphericity and angularity, and also the strength and durability.

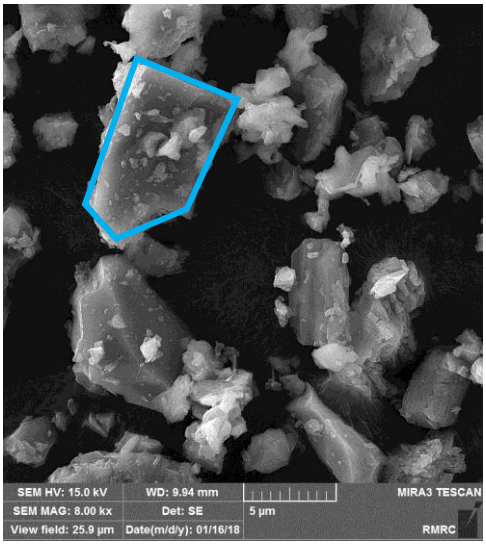

(a) Cement

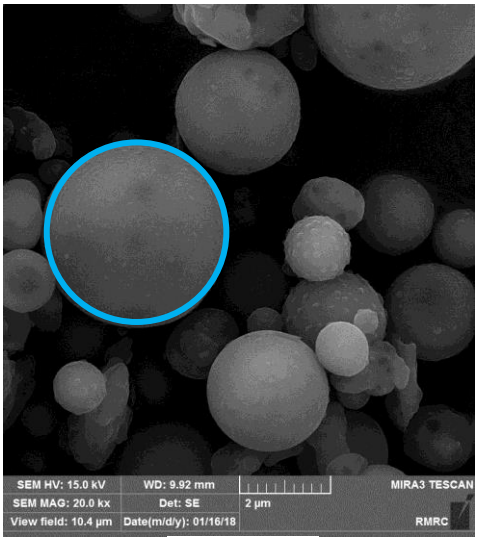

(b) FA

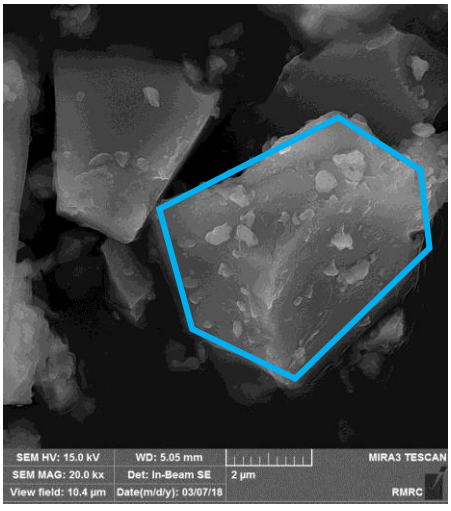

(c) Slag

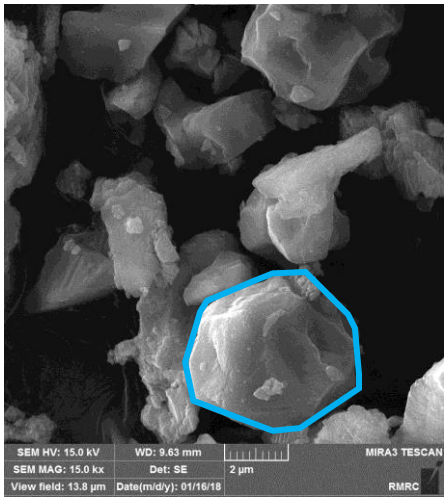

(d) LSP

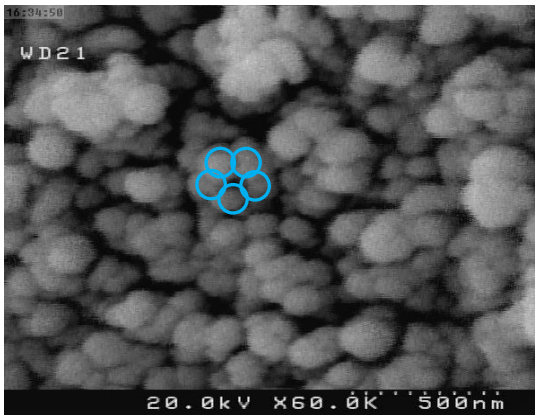

(e) NS

Fig. 16. Comparative representation of micro and nano admixtures shape in SEM micrograph

Schematic representation of the approximate shapes of the particles taken from SEM micrograph, along with their equivalent circular shapes are presented in fig. 17. In this figure, schematic comparison of particles' average size and geometry has been made. The figure demonstrates in a simple way that the admixtures' particles with less sphericity and more angularity can lead to a higher yield stress, and as a results less workability and smaller slump flow. However, it is worth mentioning that the particle size may not have a proportional effect on workability, i.e. smaller particle size does not necessarily increase the workability. For example, FA can increase the workability mora than NS does. This can, is a simple way, attributed to the fact that higher specific surface area can lead to a higher yield stress and thereby less slump flow.

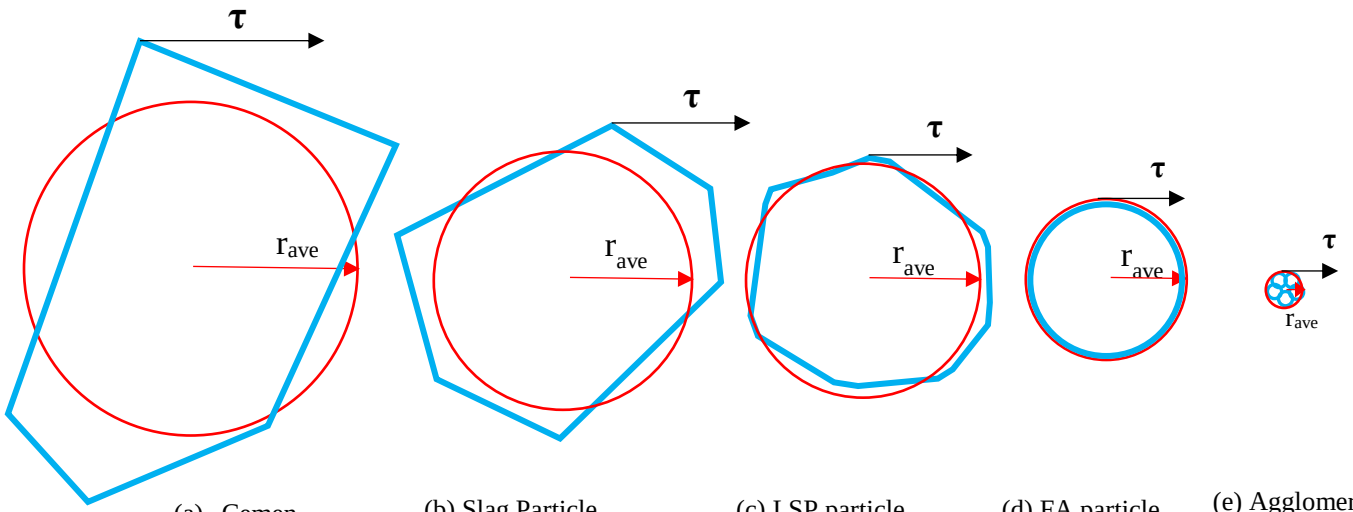

(a) Cemen (b) Slag Particle (c) LSP particle (d) FA particle (e) Agglomerate of NS particles

Fig. 17. Schematic representation of particles of micro and nano admixtures for size and shape that can be extracted from SEM micrograph

7.4.3. Virtual microstructure

Based on the approximate shape of the particles extracted from SEM images, a simplified geometry of the admixtures was considered to represent the particle sphericity and angularity in order to generate a schematic virtual microstructure using a MATLAB program. The particle size of each admixture is generated randomly using the measured particle size distribution (PSD) presented earlier, along with the mean (μ) and standard deviation (σ) calculated through Eqs. (5) and (6). This is a simplified model to generate the virtual microstructure based on the approximate particle shape of the admixtures. Particle packing model has been used by a number of researchers for strength and rheology. However, it can mostly describe the microstructure for packing and strength purpose, whereas in rheology, particle shape plays a more significant role which has been rarely investigated [31]. The schematic virtual microstructure of different blends of micro/ nano admixture are displayed in Fig. 18 which can help understand better how the combination of particles of different shape can affect the rheology in the mixture.

Fig 18a shows the cement/slag blend that has the highest angularity and the least sphericity that can thereby lead to a lower slump flow. In contrast, Fig. 18b displays the blend of cement/ LSP in which the LSP particles have more sphericity which can result in a better ball-bearing effect and skid of the particles on each other.. A perfect skidding effect can be seen in Fig. 18c which is the blend of cement/ FA due to the spherical shape of FA particles. Comparing this image with Fig. 18d that illustrates the cement/ NS blend reveals that how larger size of the particles, assuming spherical shape for both FA and NS particles, may lead to a better ball-bearing effect among the particles. As is noted, diminutiveness of NS particles can results in higher specific surface area and thereby higher stress against movement of cement particles on top of each other. Besides, it can be seen that NS particles are not large enough to separate cement particles from each other to reduce their contact and facilitate their skid on each other. However, FA particles sizes compared to cement particles are big enough to separate them and play a more efficient ball-bearing effect, i.e. easier movements of particles with less contact friction. Fig. 18e and f display denser microstructures incorporating various admixtures of different particles size without and with nanoparticles respectively. As is seen from Fig. 18e, presence of a variety of particles size and shape makes the microstructure somehow denser that can lead to more contact of particles and a little less workability compared to Fig. 18c. However, due to a more particles shape and size variety, a more

balanced interaction and contact of particles with different shapes can refine the fluid/particles microstructure and thereby leading to less bleeding and segregation. A more refined fluid/particles microstructure can be obtained by filling the fluid in the gap of coarser particles by finer particles such as NS, as depicted din Fig. 18e. As can be perceived from this figure, nanoparticles are distributed in the mixture fluid and surround the larger particles which can lead to more homogeneity and consistency of the mixture.in fact, nanoparticles provide higher contact surface area, and thereby resulting in a little higher yield stress and less chance of bleeding of the mixture.

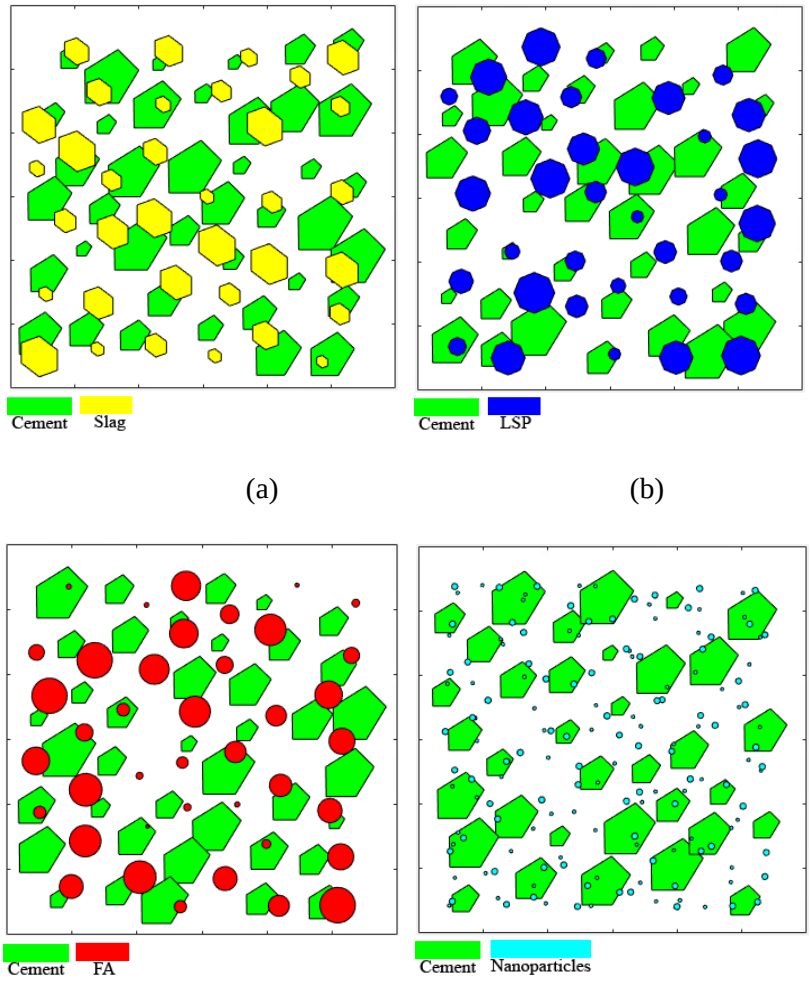

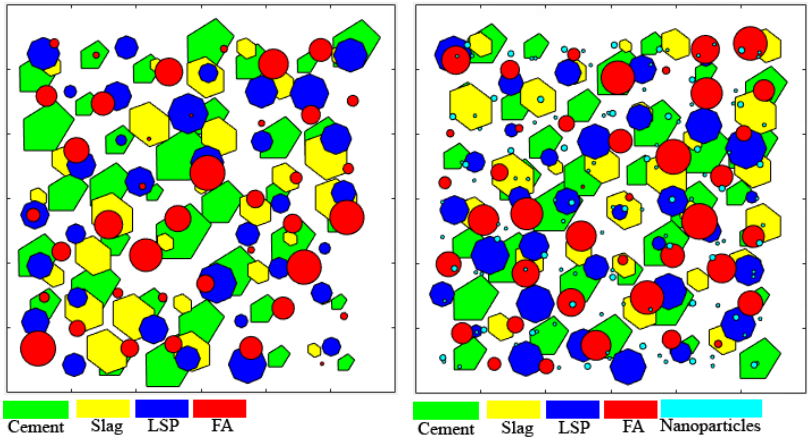

(e) (f)

Fig. 18. Virtual microstructure of different blend of admixtures

8. Conclusion

In this study, design, optimization and assessment of rheological, strength and microstructural properties of self- consolidating mortar containing micro/ nano admixtures including FA, Slag, LSP, and NS was investigated through Taguchi method. The objectives of the approach were considered to obtain practical lower w/b ratio, lower binder content, and highest cement replacement, while maintain a good rheology and optimum strength. Two phases of a performance-based design, namely A and B were considered for rheological properties for a basic mix without admixtures and a final mix incorporating micro/nano admixtures. Concurrent design of rheology and strength was considered in the phase B in order to find the optimum mix for maximum strength. It was observed that mixes with the slump flow of 23 to 28 cm had more stability, with an average of 26 cm being the most stable one. V-funnel time for the designed range was obtained as 6.4- 8.9 s with an average of 7.4 s. Based on the design objectives, it was found that the optimum replacement levels to keep the rheology in the design range was 20, 30, 10, 4% for LSP, Slag, FA, and NS, respectively. However, the optimum admixtures' levels for the highest strength were 20, 20, 20, and 4% for LSP, Slag, FA, and NS, respectively, which shows 64% cement replacement by micro/nano admixtures while enhancing the strength by about 57% compared to the basic mix. The results indicated the robustness of the design methodology and efficiency of the optimization. The microstructure of the mixes investigated through SEM also proved that the design and optimization resulted in a denser and more refined microstructure. Particle size distribution of the admixtures obtained through LPSA along with FE-SEM image of admixtures' particles were also used to investigate the microstructure in terms of particles' size and shape. It was illustrated through the virtual microstructure that how the particles size and shape

can affect the particles' skidding and movement which can affect the yield stress (slump flow) and also packing in the mixture.

References

[1] EFNARC. Specifications and guidelines for self-consolidating concrete. Surrey, UK: European Federation of Suppliers of Specialist Construction Chemicals (EFNARC); 2002.

[2] M Jalal, E Mansouri, M Sharifipour, AR Pouladkhan, " Mechanical, rheological, durability and microstructural properties of high performance self-compacting concrete containing SiO 2 micro and nanoparticles", Materials & Design, 2012; 34: 389-400.

[3] M Jalal, A Pouladkhan, OF Harandi, D Jafari, "Comparative study on effects of Class F fly ash, nano silica and silica fume on properties of high performance self compacting concrete" onstruction and Building Materials, 2015; 94, 90-104.

[4] A. Santamaría, A. Orbe, MM. Losañez, M Skaf, V Ortega-Lopez, JJ. González, Self-compacting concrete incorporating electric arc-furnace steelmaking slag as aggregate, Materials & Design, 2017; 115: 179-193.

[5] K. Amini, I. Mehdipour, S D Hwang, M. Shekarchi, Effect of binder composition on time-dependent stability and robustness characteristics of self-consolidating mortar subjected to prolonged agitation, Construction and Building Materials, 2016;112: 654–665.

[6] Md. Safiuddin , J.S. West, K.A. Soudki, Flowing ability of the mortars formulated from self-compacting concretes incorporating rice husk ash, Construction and Building Materials, 2011; 25: 973–978.

[7] HT Le, HM Ludwig, Effect of rice husk ash and other mineral admixtures on properties of self-compacting high performance concrete, Materials & Design, 2016;89: 156-166

[8] M Jalal, M Fathi, M Farzad, " Effects of fly ash and TiO2 nanoparticles on rheological, mechanical, microstructural and thermal properties of high strength self compacting concrete", Mechanics of Materials, 2013; Mechanics of Materials 61, 11-27.

[9] M Jalal, AA Ramezanianpour, MK Pool, Split tensile strength of binary blended self compacting concrete containing low volume fly ash and TiO2 nanoparticles, Composites Part B: Engineering, 2013; 55, 324-337.

[10] M Jalal, Influence of class F fly ash and silica nano-micro powder on water permeability and thermal properties of high performance cementitious composites, Science and Engineering of Composite Materials, 2013; 20 (1), 41-46.

[11] M Jalal, Corrosion resistant self-compacting concrete using micro and nano silica admixtures, Structural Engineering and Mechanics, 2014; 51 (3), 403-412.

[12] OR. Khaleel, H. Abdul Razak, The effect of powder type on the setting time and self compactability of mortar, Construction and Building Materials, 2012;36: 20–26.
[13] M. Mahdikhani, A.Akbar Ramezanianpour, New methods development for evaluation rheological properties of self-consolidating mortars, Construction and Building Materials, 2015;75: 136–143.
[14] M. Nepomuceno, L. Oliveira, SMR. Lopes, Methodology for mix design of the mortar phase of self-compacting concrete using different mineral additions in binary blends of powders, Construction and Building Materials, 2012;26: 317–326.
[15] Q. Wu, X. An, Development of a mix design method for SCC based on the rheological characteristics of paste, Construction and Building Materials, 2014;28: 642-651.
[16] WJ. Long, KH. Khayat, A. Yahia, F. Xing, Rheological approach in proportioning and evaluating prestressed self-consolidating concrete, Cement and Concrete Composites, 2017; 82:105-116.
[17] ASTM, C. "128-07a." Standard test method for density, relative density (specific gravity), and absorption of fine aggregate, 2008.
[18] ASTM C 125. Standard Terminology Relating to Concrete and Concrete Aggregates, 2005.
[19] Singh S., Shan H. S., Kumar P.; Parametric Optimization of Magnetic-Field- Assisted Abrasive Flow Machining by the Taguchi Method, Quality and Reliability Engineering International, pp. 273- 283, 2002.
[20] Ross P. J.; Taguchi Techniques for Quality Engineering. Mcgraw-Hill International Editions, ISBN 0-07-114663-6. p. 329, 1996.
[21] Dubey A. K., Yadava V.; Simultaneous Optimization of Multiple Quality Characteristics in Laser Beam Cutting Using Taguchi Method. International Journal of Precision Engineering and Manufacturing. Vol 8. No.4, 2007, pp. 10-15.
[22] Z. Tan. SA. Bernal . JL. Provis, Reproducible mini-slump test procedure for measuring the yield stress of cementitious pastes, Materials and Structures, 2017; 50:235.
[23] A. Bouvet, E. Ghorbel., R. Bennacer, The mini-conical slump flow test: Analysis and numerical study, Cement and Concrete Research, 2010;40: 1517–1523.
[24] A.W. Saak, H.M. Jennings, S.P. Shah, New methodology for designing selfcompacting concrete, ACI Materials Journal 98 (6) (2001) 429–439.
[25] N. Roussel, P. Coussot, Fifty-cent rheometer for yield stress measurements: from slump to spreading flow, Journal of Rheology 49 (3) (2005) 705–718.
[26] M. Benaicha, Y. Burtschell, AH. Alaoui, K. Elharrouni, Theoretical calculation of self-compacting concrete plastic viscosity, Structural Concrete. 2017;1–10.
[27] T. Bouziani, A. Benmounah, Correlation Between V-funnel and Mini-slump Test Results with Viscosity, KSCE Journal of Civil Engineering, 2017; 17(1):173-178.

[28] N. Tregger, L. Ferrara, S P. Shah, Identifying Viscosity of Cement Paste from Mini-Slump-Flow Test, ACI MATERIALS JOURNAL, 2008, 558-566.

[29] ASTM C1611 / C1611M-14, Standard Test Method for Slump Flow of Self-Consolidating Concrete, ASTM International, West Conshohocken, PA, 2014, www.astm.org

[30] A. Arora, M. Aguayo, H. Hansen, C. Castro, E. Federspiel, B. Mobasher, N. Neithalath, Microstructural packing- and rheology-based binder selection and characterization for Ultra-high Performance Concrete (UHPC), Cement and Concrete Research, 2018;103:179-190.

[31] H. Hafid, G. Ovarlez, F. Toussaint, PH. Jezequel, N. Roussel, Effect of particle morphological parameters on sand grains packing properties and rheology of model mortars, Cement and Concrete Research, 2016; 80:44-51.